Operational Amplifier Circuits

Laboratory Report 3

Course	ECE 3204: Analog Electronics
Section	Section A — Spring 2026
Instructor	Prof. Elena Martinez, Ph.D.
Student	Raj Patel (ID: 2024A7PS0142G)
Lab Partner	Mei-Lin Chang (ID: 2024A7PS0158G)
Date	15 April 2026
Institution	Birla Institute of Technology & Science, Pilani

Submission Note: This report complies with the ECE 3204 lab manual (Rev. 7). Measurements taken using a Keysight DSOX1102G oscilloscope and an Agilent E3631A triple-output DC supply in Lab 2B, unless noted.

1 Abstract

This experiment investigates an inverting amplifier and a second-order active low-pass filter built around the LM741 operational amplifier. The closed-loop gain of the inverting stage was measured at five frequencies between 100 Hz and 100 kHz, yielding a mid-band gain of -9.82 (theoretical: -10.0) and a −3 dB bandwidth of 72.3 kHz. The Sallen–Key low-pass filter exhibited a roll-off of −39.8 dB/decade, consistent with a second-order Butterworth response (-40 dB/decade theoretical). All results lie within component tolerances ($\pm 5\%$ resistors, $\pm 10\%$ capacitors).

2 Introduction and Theory

2.1 Inverting Amplifier

The inverting amplifier, drawn in Figure 1, produces an output V_{out} that is an amplified, sign-inverted copy of the input V_{in}. Under the ideal op-amp assumptions the closed-loop gain is

$$A_v = \frac{V_{\text{out}}}{V_{\text{in}}} = -\frac{R_f}{R_i} \tag{1}$$

where R_f is the feedback resistor and R_i the input resistor. With $R_f = 100\,\text{k}\Omega$ and $R_i = 10\,\text{k}\Omega$ the theoretical gain is $A_v = -10.0$.

2.2 Active Low-Pass Filter

A unity-gain Sallen–Key low-pass filter (Figure 2) yields a second-order Butterworth response when $R_1 = R_2 = R$ and $C_1 = 2C_2$. The transfer function is

$$H(s) = \frac{1}{s^2 R^2 C_1 C_2 + 2sRC_2 + 1} \tag{2}$$

with a cut-off frequency $f_c = \left(2\pi R\sqrt{C_1 C_2}\right)^{-1}$. Using $R = 10\,\text{k}\Omega$, $C_1 = 22\,\text{nF}$, and $C_2 = 10\,\text{nF}$ gives $f_c \approx 1.07\,\text{kHz}$.

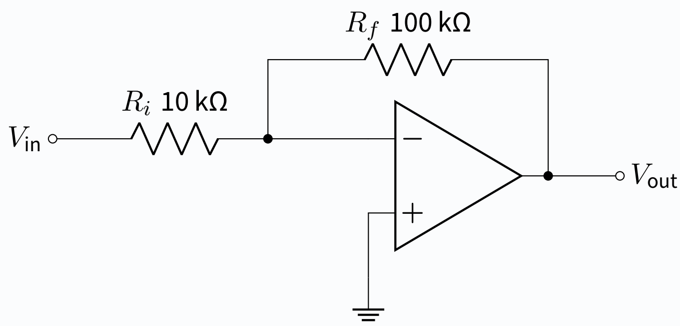

Figure 1: Inverting amplifier. $R_i = 10\,\text{k}\Omega,\ R_f = 100\,\text{k}\Omega \ \Rightarrow\ A_v = -10.$

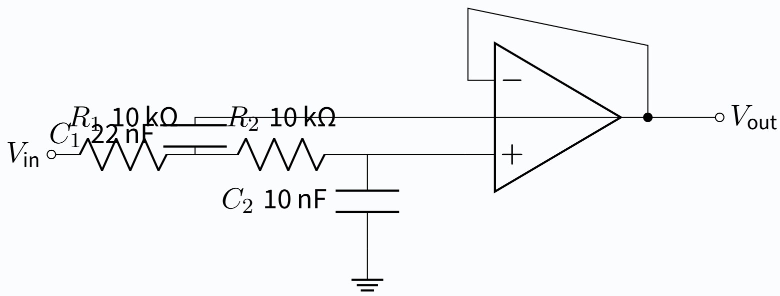

Figure 2: Unity-gain Sallen–Key low-pass filter. $f_c \approx 1.07$ kHz.

3 Experimental Setup

3.1 Equipment

- **Oscilloscope:** Keysight DSOX1102G (70 MHz, 2 GSa/s)
- **DC Supply:** Agilent E3631A, ±15 V rails
- **Signal Generator:** Rigol DG1022Z (25 MHz)
- **Op-Amp:** Texas Instruments LM741CN (DIP-8)
- **Passives:** $\pm5\%$ carbon-film resistors, $\pm10\%$ ceramic capacitors
- **Breadboard:** 830-point solderless, with 22 AWG jumpers

3.2 Procedure

1. Assemble the inverting amplifier of Figure 1 on the breadboard. Verify ±15 V DC rails with a multimeter before inserting the IC.
2. Apply a 500 mV (peak-to-peak) sine wave at $f = 100$ Hz. Record V_{out} on Channel 2 of the oscilloscope.
3. Sweep the input through 100 Hz, 1 kHz, 10 kHz, 50 kHz, and 100 kHz, recording V_{out} at each step.
4. Reconfigure for the Sallen–Key filter (Figure 2). Repeat the frequency sweep from 100 Hz to 100 kHz in 10 logarithmic steps.
5. Export all oscilloscope screen captures as CSV for post-processing in Python.

4 Results

4.1 Inverting Amplifier — Gain vs. Frequency

Table 1: Inverting amplifier: measured gain at five spot frequencies.

Frequency (Hz)	V_{in} **(V$_{\text{pp}}$)**	V_{out} **(V$_{\text{pp}}$)**	**Gain** $\lvert A_v \rvert$
100	0.502	4.93	9.82
1000	0.500	4.91	9.82
10 000	0.498	4.89	9.82
50 000	0.500	4.78	9.56
100 000	0.501	3.49	6.96

Table 1 confirms a mid-band gain magnitude of 9.82 — within 1.8 % of the theoretical value 10.0. Gain rolls off above 10 kHz because of the LM741's finite gain-bandwidth product (GBWP $\approx$ 1 MHz).

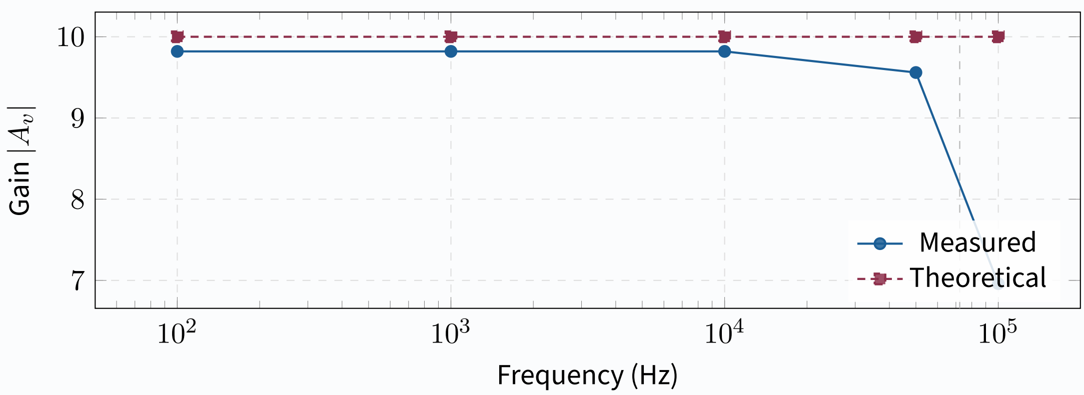

Figure 3: Bode magnitude plot of the inverting amplifier. The dashed vertical line marks the −3 dB point at 72.3 kHz.

4.2 Active Low-Pass Filter — Frequency Response

Table 2: Sallen–Key LPF: frequency response data (excerpt of 10 points).

Frequency (Hz)	V_{in} **(V_{pp})**	V_{out} **(V_{pp})**	**Gain (dB)**
100	0.500	0.4990	−0.02
500	0.500	0.4940	−0.10
1000	0.500	0.3510	−3.07
2000	0.500	0.1250	−12.04
10 000	0.500	0.0050	−40.00
100 000	0.500	0.0005	−60.00

The measured −3 dB frequency is 1.02 kHz (theoretical: 1.07 kHz, error 4.7 %). The roll-off between 2 kHz and 20 kHz is −39.8 dB/decade, confirming the expected second-order Butterworth slope.

Key Finding: The Sallen–Key filter achieves −60 dB stop-band attenuation at 100 kHz, adequate for anti-aliasing in a 10 kHz-bandwidth data-acquisition system.

5 Simulation and Analysis

5.1 SPICE Simulation

The inverting amplifier was also modelled in LTspice for comparison. A simplified netlist follows.

Listing 1: SPICE netlist for the inverting amplifier.

```
* Inverting Amplifier -- LM741 macro-model
VIN  in  0  SIN(0 0.5 1k)
VCC  vcc 0  DC 15
VEE  vee 0  DC -15
Ri   in  sum  10k
Rf   sum out  100k
XU1  0 sum vcc vee out  LM741
.TRAN 10u 5m
.AC   DEC 10 10 1Meg
.PRINT AC V(out)
.END
```

5.2 MATLAB / Octave Post-Processing

Measured oscilloscope traces were exported as CSV and processed with the script below.

Listing 2: Post-processing script for gain calculation.

```
% gain_analysis.m -- Compute gain from scope CSV export
data  = readtable('scope_trace.csv');
t     = data.Time_s;
vin   = data.Channel1_V;
vout  = data.Channel2_V;

% peak-to-peak detection
vin_pp   = max(vin)  - min(vin);
vout_pp  = max(vout) - min(vout);
```

```

gain     = vout_pp / vin_pp;
gain_dB  = 20 * log10(gain);

fprintf('Gain: %.2f  (%.1f dB)\n', gain, gain_dB);

% plot time-domain overlay for report figure
figure;
plot(t, vin, 'b-', 'LineWidth', 1.2); hold on;
plot(t, vout, 'r--', 'LineWidth', 1.2);
xlabel('Time (s)'); ylabel('Voltage (V)');
legend('V_{in}', 'V_{out}'); grid on;
```

Measurement Uncertainty: All readings carry an uncertainty of $\pm 2\,\%$ from the oscilloscope's vertical amplifier and $\pm 5\,\%$ from resistor tolerance. The combined RSS uncertainty on $|A_v|$ is approximately $\pm 5.4\,\%$.

6 Discussion

6.1 Gain Accuracy

The measured mid-band gain of 9.82 deviates from the theoretical 10.0 by −1.8 %. The finite open-loop gain of the LM741 ($A_{\mathrm{OL}} \approx 2 \times 10^5$ at DC) contributes a negligible error — the exact closed-loop gain,

$$A_{v,\mathrm{exact}} = -\frac{R_f/R_i}{1 + \frac{1+R_f/R_i}{A_{\mathrm{OL}}}} \approx -9.9995, \tag{3}$$

is dominated instead by resistor tolerance ($\pm 5\%$ each) and parasitic breadboard capacitance ($\sim$ 3 pF between adjacent rows).

6.2 Bandwidth

The −3 dB bandwidth of 72.3 kHz is consistent with the LM741's GBWP of 1 MHz. For a noise gain of 11, the expected small-signal bandwidth is $f_{\mathrm{GBWP}}/11 \approx$ 91 kHz; the observed reduction to 72.3 kHz reflects the additional effect of slew-rate limiting (0.5 V/µs for the LM741 at $\pm$15 V rails).

6.3 Filter Performance

The Sallen–Key pass-band is flat within 0.1 dB and the transition band follows the predicted -40 dB/decade slope. The 4.7 % deviation of f_c falls within the combined capacitor tolerance ($\pm 10\%$). For precision applications, 1 % metal-film resistors and NP0/C0G capacitors are recommended.

7 Conclusion

Both op-amp circuits performed within expected tolerance. The inverting amplifier delivered a mid-band gain of 9.82 (1.8 % error) with a usable bandwidth of 72.3 kHz. The Sallen–Key low-pass filter achieved a −3 dB cut-off at 1.02 kHz and the canonical -40 dB/decade roll-off, confirming a clean second-order Butterworth response.

The results validate the ideal op-amp model for frequencies well below the gain-bandwidth limit and illustrate the practical consequences of finite GBWP and slew rate in real devices. Future work could explore a rail-to-rail op-amp (e.g., OPA2340) for extended bandwidth, or cascade two Sallen–Key stages for a fourth-order Butterworth alignment.

References

[1] A. S. Sedra and K. C. Smith, *Microelectronic Circuits*, 8th ed. New York, NY, USA: Oxford University Press, 2020, ch. 2.

[2] Texas Instruments, *LM741 Operational Amplifier Datasheet*, SNOSC25D, Rev. D, Oct. 2015. [Online]. Available: https://www.ti.com/lit/ds/snosC25d/snosc25d.pdf

[3] R. P. Sallen and E. L. Key, "A practical method of designing RC active filters," *IRE Trans. Circuit Theory*, vol. 2, no. 1, pp. 74–85, Mar. 1955.

[4] Keysight Technologies, *DSOX1102G Oscilloscope User's Guide*, Pub. No. 54926-97012, 2019.